

Original Article

Ste20 is crucial for dimorphic switching of *sporothrix schenckii* and affects its global transcriptome

Binbin Hou¹, Zhenying Zhang², Jiaorui Zhou³, Fangliang Zheng⁴, Ming Li³

¹Department of Dermatology, The Second Hospital of Dalian Medical University, Dalian, China; ²Department of Dermatology, University of Hong Kong-Shenzhen Hospital, Shenzhen, China; ³Department of Microecology, College of Basic Medical Science, Dalian Medical University, China; ⁴Liaoning University, Shenyang, Liaoning, China

Received January 1, 2020; Accepted February 6, 2020; Epub March 1, 2020; Published March 15, 2020

Abstract: *Sporothrix schenckii* induced sporotrichosis has gained importance in recent years because of its worldwide prevalence. The dimorphic switching process is required for the pathogenesis of *S. schenckii*. Previously, we found that STE20-like protein kinase (SsSte20) was overexpressed in the early yeast stage, but not in the mycelial stage of *S. schenckii*, which suggested its involvement in morphogenesis of this fungal pathogen. It remains unclear, however, whether SsSte20 is essential for dimorphic switching of *S. schenckii* and what are its related genes. In this study, the function of SsSte20 was investigated using double-stranded RNA interference (dsRNAi) mediated by *Agrobacterium tumefaciens*. We evaluated its effects on normal asexual development, yeast-phase cell formation, and cell wall composition and integrity. In addition, by transcriptome analysis of the SsSte20 knockdown (SsSte20-i) mutant and the standard *S. schenckii* strain, we further investigated the genes and pathways that were affected by SsSte20. Our results showed that inactivation of SsSte20 significantly affected the growth and internal components of *S. schenckii* conidia and impaired the dimorphic switching process. RNA transcriptome analysis of the standard *S. schenckii* strain and the SsSte20-i mutant revealed that SsSte20 inhibition affected the genes that were not only involved in the biological process, but also in the cellular component, and the molecular functions of *S. schenckii*. It mainly affected the expression of iron/ion-binding transporter genes, oxidation-reduction-related genes, 1, 3-beta-glucosidase, and methylsterol monooxygenase, which are highly associated with environmental information processing and the biosynthesis of cell wall components. Overall, our research supports the claim that SsSte20 plays an essential role in the dimorphism of *S. schenckii* and affects its global transcriptome.

Keywords: Ste20, sporotrichosis, *sporothrix schenckii*, dimorphic switching, transcriptome

Introduction

Sporotrichosis, an endemic mycosis caused by species of *S. schenckii*, has gained importance in recent years because of its worldwide prevalence, especially in Brazil, China, and South Africa [1, 2]. *S. sporotrichosis* can cause chronic infection of the skin, subcutaneous tissue, and nearby lymphatic vessels, resulting in pus, ulceration, and exudation, which induce further damage to the muscles, bones, central nervous system, and other organs [2-4]. The morphologic switch from the mold form to the yeast form occurs when filamentous *S. schenckii* adapts to a novel niche and infects a mammalian host, and this mode of transmission, known as dimorphic switching, is obligatory for establishing its pathogenicity [5]. Understanding the biology that determines dimorphic switching

may aid in the development of novel strategies to effectively manage sporotrichosis.

Dimorphic switching is a tightly regulated process in pathogenic fungi, which involves a number of signaling pathways, including two-component and heterotrimeric G protein-signaling systems, as well as Ras and cAMP signaling and the downstream mitogen-activated protein kinase (MAPK) cascade [6-9]. Among them, the Ras signaling pathway has been shown to influence not only the dimorphic switching and adaptation to oxidative stress in dimorphic fungi but also the asexual development and conidial germination [10-13]. The p21-activated kinase, Ste20, is a key component of the Ras signaling pathway, in which Ras activates the Rho GTPase Cdc42, which regulates Ste20 and Cla4 to signal by MAPK pathways and control cell division

Ste20 is required for pathogenesis in *sporothrix schenckii*

[14-16]. Previously, by using two-dimensional electrophoresis, we identified that STE20-like protein kinase (SsSte20) was overexpressed in the early yeast stage but not in the mycelial stage of *S. schenckii* [17, 18], which suggested its involvement in the morphogenesis and pathogenesis of this fungal pathogen [19]. It remains unclear, however, whether SsSte20 can respond to temperature changes and affect the dimorphic switching of *S. schenckii*, and what are its downstream target genes. RNAi technology was used to corroborate the role of calcium/calmodulin kinase I in *S. schenckii* dimorphism. Yeast cells were transformed with the pSilent-Dual2G (pSD2G) plasmid with or without inserts of the coding region of the calcium/calmodulin kinase I (sscmk1) gene [20].

In this study, we investigated the function of SsSte20 using double-stranded RNA interference (dsRNAi) mediated by *Agrobacterium tumefaciens*. We evaluated its effects on normal asexual development, yeast-phase cell formation, and cell wall composition and integrity. In addition, by transcriptome analysis of the SsSte20 knockdown (SsSte20-i) mutant and the standard *S. schenckii* strain, we further investigated the response genes affected by SsSte20 and elucidated the possible correlation of these genes with the dimorphism and virulence of *S. schenckii*.

Materials and methods

Fungal strains and culture conditions

Strain *S. schenckii* ATCC10268, maintained in the Research Center for Pathogenic Fungi of Dalian Medical University (Dalian, China), was used as the standard strain, as well as for the construction of the SsSte20 RNA interference mutant. The mycelial and yeast colonies of *S. schenckii* were cultured in sabouraud dextrose agar (SDA) medium at 25°C and in liquid BHI medium (Hyclone; GE Healthcare Life Sciences, Logan, UT, USA) at 37°C, PH 7. The mycelial colonies of *S. schenckii* ATCC10268 [21] were transferred to liquid BHI medium at 37°C with sterilization ring and agitated at 100 rpm for 96 h to achieve a switch from the mycelial to the yeast phase. The *Agrobacterium tumefaciens* EHA105 strain was cultured in lysogeny broth (LB) medium supplemented with 50 µg/ml kanamycin and 20 µg/ml rifampicin at 28°C to

maintain the plasmids. For RNA interference, 200 µmol acetosyringone was added as an inducer to the inductive medium containing agar 15 g/l, K-buffer 8 ml/l, Mn-buffer 20 ml/l, 1% CaCl₂·2H₂O 1 ml/l, 0.01% FeSO₄ 10 ml/l, 20% NH₄NO₃ 2.5 ml/l, 50% glycerine 10 ml/l, 1 M 2-(N-morpholino) ethanesulfonic acid 40 ml/l, 20% glucose 10 ml/l. Hygromycin (100 mg/l) and cefotaxime (200 µM) were also added to the inductive medium to screen the SsSte20-interference isolates. For the cell wall test, strains were grown for 5 days at 25°C on SDA medium with 20 µg/ml Congo red. To test resistance to zymolyase, strains were grown on SDA medium with 100 µl zymolyase 20T (10 mg/ml in 10 mM Tris/HCl, pH 7.5; Sigma-Aldrich; Germany) at 25°C for 30 h [22].

Plasmid construction

The SsSte20 gene was PCR amplified from the *S. schenckii* genomic cDNA using the following primers. STE20-F: 5'-CGGGGTACCCTCGAGTTG-CAGCTCCAAGCACAAAC-3' with designed KpnI and XhoI endonuclease sites, STE20-R: 5'-GAA-GATCTAAGCTTCAGTGAGTTTGCCTCGGTAC-3' with designed BglII and HindIII endonuclease sites. The enzyme digested PCR amplicon was ligated into pCB309 plasmid synthesized from pSilent-1 (the Fungal Genetics Stock Center, Manhattan, KS, USA) to construct the final SsSte20 double stranded RNA interference (dsRNAi) plasmid, pCB309-pfgrt [21]. It contained a 540 bp fragment of SsSte20 sequence hairpin repeats under the control of the fungal PtrpC promoter, and the hygromycin resistance gene marker. pCB309 plasmids lacking the SsSte20 hairpin repeat sequence were used as a control (Ste20-control group).

Construction of SsSte20 interference (SsSte20-i) mutant

The transformation procedure was performed as previously described [21]. *A. tumefaciens* containing pCB309-pfgrt with the transfer T-DNA fragment was incubated in LB medium with kanamycin and rifampicin for 48 h at 28°C. *S. schenckii* conidia were grown in the BHI medium. Following washing with sterile water, the conidia (5×10⁶ CFU/ml) and *A. tumefaciens* containing PCB309-pfgrt were mixed in the inductive medium. The transformants were selected on medium containing hygromycin (100 mg/l) and cefotaxime (200 µM). The mycelial

Ste20 is required for pathogenesis in *sporothrix schenckii*

dry weight of the standard strain, SsSte20-i strain, and wide type strain were detected by centrifugation of the cultures at 4°C for 30 min at a speed of 20,000×g, followed by drying at 60°C overnight.

Morphologic observation by transmission electron microscopy (TEM) and scanning electron microscopy (SEM)

Electron micrographs were generated using a JEOL JEM-2000EX electron microscope (JEOL Ltd., Tokyo, Japan) after the fungal samples were prepared as previously described by [23]. Standard strains and wild-type strains were cultured at 25°C SDA medium and 37°C BHI medium respectively. Colonies were selected and made into specimens for transmission electron microscopy (TEM) and scanning electron microscopy (SEM) observation. For scanning electron microscope, the samples were prepared using a method previously described [24]. Samples were immersed in 2% glutaraldehyde for 2 hours, washed twice with sodium dimethylarsenate detergent, and immersed in 1% osmium acid for 2 hours. Then gradient dehydration was carried out with alcohol. The intermediate solution was replaced and dried. Dried colonies were coated with platinum-vanadium and observed under a QUANTA 450 scanning electron microscope (FEI; Thermo Fisher Scientific, Inc., Hillsboro, OR, USA) at an accelerating voltage of 20.0 kV.

Total RNA isolation, library construction, and sequencing

Total RNA for Illumina sequencing was extracted from the standard and SsSte20-i strains grown at 37°C using a Trizol Bacterial RNA Isolation Kit (Thermo Fisher) according to the manufacturer's protocol. During RNA isolation, DNA was removed by treating the samples with RNase-free DNase (Solarbio) for 30 min at 37°C to avoid DNA contamination. The purity, concentration, and integrity of the RNA were examined using a NanoPhotometer spectrophotometer (IMPLEN, CA, USA), Qubit 2.0 fluorometer (Life Technologies, CA, USA) and an Agilent Bioanalyzer 2100 system (Agilent Technologies, CA, USA). The library construction and sequencing were performed by the Allwegene-BioTech in Beijing (China) as described previously [25]. The processed reads were mapped to the *S. schenckii* 1099-18 genome assembly

using TopHat 2.1.18 with reference annotation. FPKM values for each gene and differentially expressed genes (DEGs) were analyzed with Cufflinks v2.2.131. The differentially expressed genes between two samples were identified considering both fold change and q-value. DEGs between the standard and SsSte20-i cells used a model based on the negative binomial distribution with an absolute value of \log_2 (fold change) >1.5 and an adjusted *P*-value <0.05.

Gene ontology (GO) enrichment analysis of differentially expressed genes

The DEGs were used for Gene Ontology (GO) enrichment analysis to help further understand the biologic functions of the identified genes and significantly enriched metabolic pathways. In this study, both GO terms with adjusted *P*-value <0.05 were considered significantly enriched in DEGs.

Statistical analysis

Data are presented as the mean ± standard deviation. The graphpad prism (version 5.0) software was used for statistical analysis. *P*< 0.05 was considered to indicate a significant difference.

Results

dsRNAi for SsSte20 in S. schenckii

We constructed the SsSte20-i strain using dsRNAi mediated by *A. tumefaciens* as indicated in the "Materials and Methods" section. To assay the silencing efficiency, we performed quantitative real-time PCR (qPCR) analysis to evaluate the SsSte20 gene expression. Results showed that the transcription level of SsSte20 mRNA was about 24.38% of that in the standard strain at 25°C, but when it was grown at 37°C, the expression of SsSte20 mRNA increased significantly (more than tenfold) in the standard strain, but not in the SsSte20-i mutant, which suggested that dsRNAi silencing was stable and efficient (**Figure 1**).

Inactivation of SsSte20 impaired the dimorphic switching of S. schenckii

When cultured in solid *sabouraud* dextrose agar (SDA) medium at 25°C, the SsSte20-i strain exhibited an obvious reduction in colony

Ste20 is required for pathogenesis in *sporothrix schenckii*

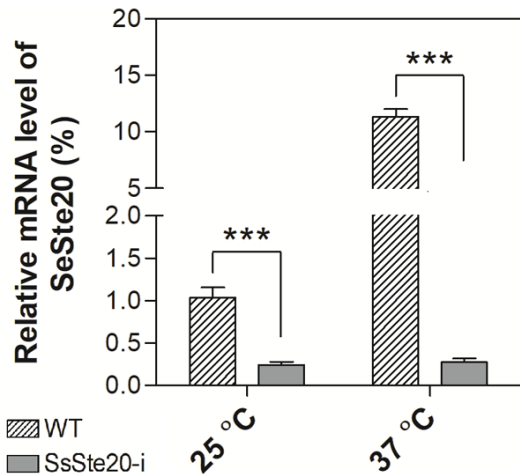


Figure 1. The mRNA expression level of SsSte20 in the standard and SsSte20-i strains cultured at 25°C and 37°C, respectively. Values are expressed as mean \pm SD, n=3. ***P<0.001.

size and pigment production compared with a wild type (WT) strain isolated from a patient. The wild type strain produced the most pigment and the SsSte20-i strain had the smallest colony growth diameter (**Figure 2A**). When cultured in liquid medium, growth of the SsSte20-i strain was markedly impaired either in SDA medium at 25°C or in brain heart infusion (BHI) liquid medium at 37°C. When growing at 25°C, it can be seen from the curve that the hyphal dry weight of the SsSte20-i strain is the lowest; the difference between the wild strain and the standard strain is not significant. When growing at 37°C, the OD value of the SsSte20-i strain is the lowest, while the difference between the wild strain and the standard strain is not significant, (All P<0.001; **Figure 2B**), compared with that of the WT and standard strains. The standard strain displayed dense and round conidia at the tips of the hyphae (**Figure 2C**), whereas the SsSte20-i strain showed only scarce and wizened conidia.

Inactivation of SsSte20 affected the internal components of S. schenckii conidia

To observe the detailed morphologic change in the SsSte20-i strain during dimorphic switching, we cultured this strain and the standard strain at 25°C and 37°C, respectively, and examined the strains under a scanning electron microscope. At 25°C, the mycelial phase consisted mainly of slender mycelia and round spores, while the yeast phase consisted mainly

of round spores at 37°C. SsSte20-i strain, when cultured at 25°C or 37°C, mycelia and spores were dominant. The SsSte20-i strain demonstrated smooth hyphae with less invaginations compared with the standard strain (**Figure 3A**), which switched into multiple spores at 37°C. In contrast, the SsSte20-i strain showed similar morphology at both temperatures. By transmission electron microscopy, we further observed the structure of SsSte20-i cells. When cultured at 25°C, standard strain was consisted with slender hyphae, clear inner structure, thick and complete cell wall, and at 37°C mainly round spores. The inner structure of the strain was clear; the cell wall was thick and complete. But in the SsSte20-i strain, 25°C or 37°C, mycelia and spores are dominant, mycelium length is shorter than the standard strain; spores also become ellipse shaped, the internal structure of mycelia and spores is disordered, and the cell wall has relative integrity. Results showed that slender mycelia of the standard strain at 25°C had clear, thicker, and intact cell walls (**Figure 3B, 3C**), and the yeast phase at 37°C was dominated by round spores with a clear inner cell structure and thick cell wall. At both temperatures, however, the SsSte20-i strain demonstrated short hyphae with chaotic inner structures.

Differentially expressed genes in the SsSte20-i strain compared with the standard strain when cultured at 37°C

To investigate the effects of SsSte20 on the expression of other genes in *S. schenckii*, the entire RNA transcriptome of the SsSte20-i strain was compared with that of the standard strain. The RNA used for library construction had to pass the quantity and quality control criteria. We constructed the libraries from these two different strains and produced raw reads using the Illumina HiSeq sequencing platform (San Diego, CA, USA). A total of 108.83 M clean reads, and 16.38 Gb clean bases per sample were generated by RNAseq (**Table 1**). These reads were mapped to the complete reference genome of the *S. schenckii* 1099-18 strain. On average, 95.49% of the clean reads were uniquely mapped to the reference genome.

We determined differentially expressed genes (DEGs) using the DESeqR package based on the criteria of \log_2 (fold change) >1.5 and adjusted P-value <0.05 (**Table 2**). At 37°C, 117

Ste20 is required for pathogenesis in *sporothrix schenckii*

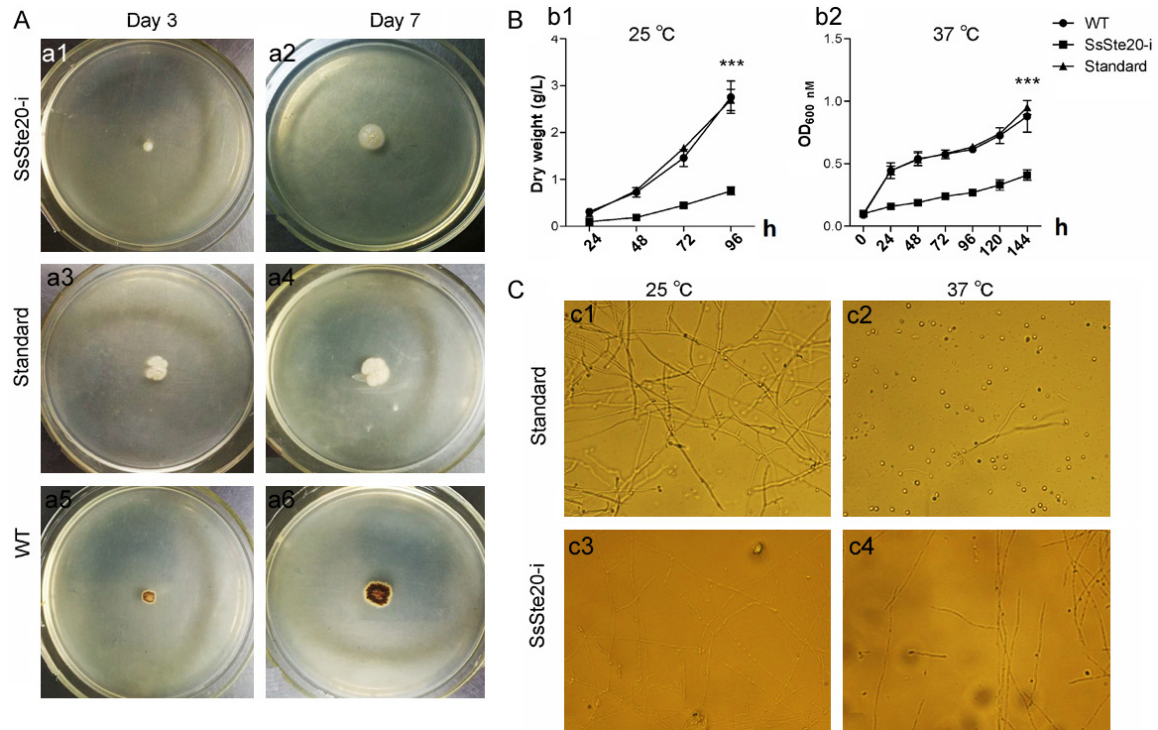


Figure 2. The morphology and growth of the SsSte20-i mutant compared with the WT and standard strains. A. Colony morphology of different strains cultured at 25°C; B. Dry weight of the mycelium and optical density (OD) values of conidia from different strains cultured at 25°C and 37°C, respectively; C. WT, standard, and SsSte20-i strains visualized under a microscope, with conidia formation at the tips and along the hyphae indicated by black arrowheads. Values are expressed as mean \pm SD, n=3. ***P<0.001.

genes were up-regulated and 130 genes were down-regulated in the standard strain compared with the SsSte20-i strain (Figure 4A). We found some of these genes to be significantly up-regulated or down-regulated when evaluated by FDR and fold change analysis (Figure 4B). They included formate dehydrogenase (SPSK_02444), HPP family protein (SPSK_09455), phosphotransferase enzyme family protein (SPSK_09552), S-(hydroxymethyl)glutathione dehydrogenase (SPSK_05312), and prostaglandin-endoperoxide synthase 1 (SPSK_03862), which are involved in metabolic pathways, including glyoxylate and dicarboxylate metabolism, methane metabolism, and biosynthesis of secondary metabolites. Moreover, Glycosylphosphatidylinositol (GPI)-anchor transamidase precursor (SPSK_09357), 3-ketosphinganine reductase (SPSK_03570), and transporter proteins, such as inorganic phosphate transporter (SPSK_04818) and ABC transporters (SPSK_04818), were found to be significantly down-regulated, which provided evidence that the meiosis and sphingolipid metabolism process-

es were affected by inactivation of SsSte20 (https://www.ncbi.nlm.nih.gov/genome/22522?genome_assembly_id=228759. https://www.ncbi.nlm.nih.gov/assembly/GCF_000961545.1/#/def).

Functional annotation of the transcriptome of the SsSte20-i strain and the standard strain

To functionally analyze the SsSte20-i transcriptome, we performed a Gene Ontology (GO) enrichment analysis of the DEGs. The GO terms from hierarchical vocabularies, describing biological processes, cellular components, and molecular functions, to analyze the transcripts, were allocated using Blast2GO software [26]. The results showed that 247 DEGs were assigned to the biological process category, and 148 DEGs and 147 DEGs were assigned to the cellular component and molecular function categories, respectively (Figure 5A). These DEGs were assigned to many GO terms, and we found that the genes related to the cellular component, especially those related to the membrane part and the intrinsic/integral component of

Ste20 is required for pathogenesis in *sporothrix schenckii*

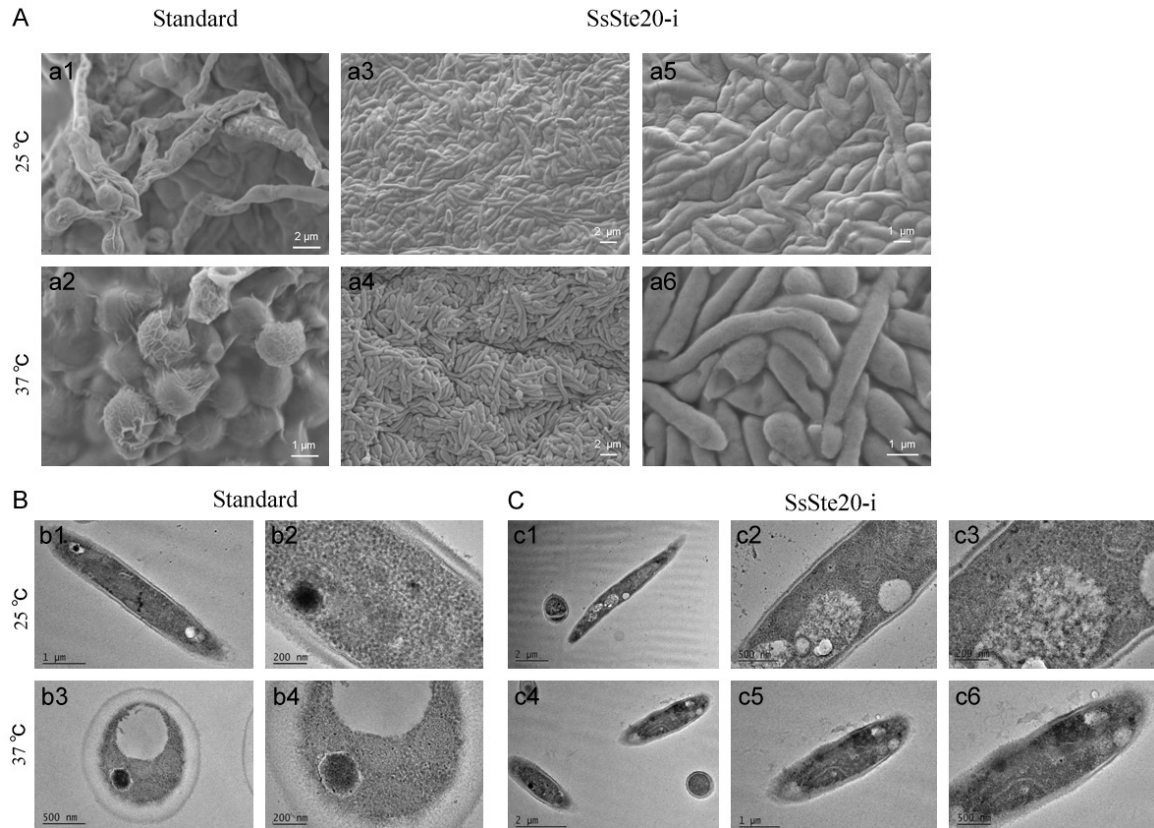


Figure 3. A. Hyphal and conidial sections of standard and SsSte20-i strains were observed by transmission electron microscopy. At 25 °C, standard strain consisted mainly of slender hyphae and round spores. At 37 °C it mainly consisted of round spores. But the SsSte20-i strains, mycelia and spores all can be seen; the difference was not significant, at 25 °C or 37 °C. B and C. The structures of SsSte20-i and standard cells were observed by transmission electron microscopy, when cultured at 25 °C and 37 °C, respectively. At 25 °C, the standard strain was dominated by slender hyphae and at 37 °C, by round spores. The internal structure of the bacteria was clear, with thick and complete cell walls; SsSte20-i strains were dominated by mycelium and spore-based, mycelium length shorter than the standard strain at 25 °C, 37 °C, mycelium became to long round spores-based, the internal structures of the bacteria are disordered, and the cell wall is incomplete.

Table 1. RNA-seq data statistics

Sample group	Clean Reads (M) ^a	Clean Bases (G) ^b	Q20 (%) ^c	Q30 (%) ^d	GC (%) ^e	Read Length (bp)
Standard	111.6901	16.8652	97.43	93.44	55.76	151
SsSte20-i	105.2715	15.8960	97.56	93.77	54.27	151

^aReads from sequencing after filtering low-quality reads. ^bThe number of clean reads is multiplied by the length and converted to G. ^cQ20, the percentage of bases with a Phred value >20. ^dQ30, the percentage of bases with a Phred value >30. ^eGC (%), percent of G and C bases.

the peroxisomal membrane, were significantly down-regulated in the SsSte20-i strain (**Figure 5B**). In contrast, the genes related to the cell or intracellular part were not affected. Also, some of the DEGs that were involved in the biological process and molecular function of *S. schenckii* were up-regulated (**Figure S1**). The terms and genes from the function ontology that were significantly different between the standard and SsSte20-i strains are listed in **Table 3**.

Discussion

Although sporotrichosis currently is regarded as an emergent disease in several countries, the factors driving its pathogenesis are still largely unknown. This has hampered the medical control of the disease [3]. Similar to other pathogenic fungi, such as *Penicillium marneffei*, the ability of *S. schenckii* to switch between a multicellular hyphal form and a unicellular

Ste20 is required for pathogenesis in *Sporothrix schenckii*

Table 2. List of up and down-regulated genes in SsSte20-i compared with the standard strain when cultured at 37 °C

GeneID	Length	Log ₂ Fold Change (Ste20-i/Standard)	P value	FDR	Up/Down Regulation	Description
27664592	1098	4.587368957	0	0	Up	[SPSK_02444] formate dehydrogenase
27667431	1056	4.137503524	2.21E-24	3.94E-23	Up	[SPSK_05406] alcohol dehydrogenase, propanol-preferring
27667341	1299	3.948161068	2.24E-27	4.58E-26	Up	[SPSK_05315] salicylate hydroxylase
27663453	816	3.158201499	2.11E-129	2.38E-127	Up	[SPSK_01245] solute carrier family 25 (mitochondrial adenine nucleotide translocator)
27672073	1710	2.353035863	2.32E-69	1.37E-67	Up	[SPSK_10337] amidase
27669349	1551	2.288244969	8.53E-05	0.000312385	Up	[SPSK_07409] pantothenate transporter
27662426	729	2.266329485	4.33E-06	1.94E-05	Up	[SPSK_00169] glutathione S-transferase
27671304	1131	2.0490202	1.70E-282	4.82E-280	Up	[SPSK_09455] HPP family protein
27669206	1794	1.995986937	2.71E-06	1.26E-05	Up	[SPSK_07265] siderophore iron transporter
27665691	810	1.78251175	6.29E-21	9.28E-20	Up	[SPSK_03577] esterase
27663784	1827	1.651073641	1.02E-132	1.24E-130	Up	[SPSK_01598] stress-induced-phosphoprotein 1
27671489	915	1.641344971	2.09E-13	1.93E-12	Up	[SPSK_09640] THO complex subunit 4
27662408	1059	1.638204522	2.68E-06	1.24E-05	Up	[SPSK_00151] hscarg dehydrogenase
27672551	1161	1.637585108	8.90E-22	1.36E-20	Up	[SPSK_11056] cytochrome b
27664575	1470	1.630316178	1.03E-05	4.38E-05	Up	[SPSK_02426] lysine 2,3-aminomutase
27672547	1464	1.503020887	2.63E-08	1.56E-07	Up	[SPSK_11052] NADH dehydrogenase subunit 4
27671208	1236	-11.10754403	7.09E-218	1.73E-215	Down	[SPSK_09357] GPI-anchor transamidase precursor
27665684	822	-7.060695932	7.69E-05	0.000283672	Down	[SPSK_03570] 3-ketosphinganine reductase
27665323	1728	-3.849682046	0	0	Down	[SPSK_03205] MFS transporter, PHS family, inorganic phosphate transporter
27663783	1491	-3.839327312	7.64E-17	8.93E-16	Down	[SPSK_01597] MFS transporter, DHA1 family, multidrug resistance protein
27663932	1161	-3.026967048	6.90E-07	3.45E-06	Down	[SPSK_01749] 2-hydroxyacid dehydrogenase
27672143	525	-2.570880084	1.82E-34	5.08E-33	Down	[SPSK_10468] solute carrier family 31 (copper transporter), member 1
27663245	1980	-2.370698319	0	0	Down	[SPSK_01037] malate dehydrogenase (oxaloacetate-decarboxylating) (NADP+)
27662967	1911	-2.354974996	8.64E-16	9.41E-15	Down	[SPSK_00742] ferric-chelate reductase
27669838	648	-2.202175461	8.26E-85	5.72E-83	Down	[SPSK_07908] superoxide dismutase, Fe-Mn family
27669783	870	-2.158890951	1.88E-11	1.48E-10	Down	[SPSK_07853] class II aldolase/adducin domain protein
27669193	1728	-2.104992766	1.81E-48	7.15E-47	Down	[SPSK_07252] NADPH oxidase
27669672	1038	-2.039663091	3.69E-131	4.27E-129	Down	[SPSK_07738] thiamine biosynthetic enzyme
27664428	2277	-2.036464326	3.40E-22	5.35E-21	Down	[SPSK_02279] metalloredutase
27669705	542	-1.987983983	1.07E-108	9.88E-107	Down	[SPSK_07772] short-chain dehydrogenase
27665475	1347	-1.924551321	5.95E-25	1.10E-23	Down	[SPSK_03360] MFS monocarboxylate transporter
27667950	1849	-1.846678464	0	0	Down	[SPSK_05965] urea transport protein
27670875	1599	-1.725188426	1.51E-206	3.17E-204	Down	[SPSK_09017] 2-oxoisovalerate dehydrogenase E2 component (dihydropolyltransacylase)
27670817	1758	-1.725170372	4.51E-42	1.51E-40	Down	[SPSK_08957] amidase
27671169	1281	-1.66783448	2.31E-271	6.16E-269	Down	[SPSK_09318] branched-chain amino acid aminotransferase

Ste20 is required for pathogenesis in *Sporothrix schenckii*

27669629	1041	-1.66238653	1.17E-33	3.18E-32	Down	[SPSK_07695] oxidoreductase, 2OG-Fe (II) oxygenase family
27663349	1422	-1.601097879	3.11E-146	4.27E-144	Down	[SPSK_01141] isopenicillin N epimerase
27662392	1350	-1.590508426	1.95E-21	2.95E-20	Down	[SPSK_00135] fumarylacetoacetase
27668443	999	-1.578487349	7.46E-168	1.17E-165	Down	[SPSK_06460] inositol oxygenase
27668333	1224	-1.537065011	3.21E-51	1.34E-49	Down	[SPSK_06350] aspergillopepsin I
27668069	1797	-1.536613527	2.08E-264	5.39E-262	Down	[SPSK_06084] 1-pyrroline-5-carboxylate dehydrogenase
27671077	1326	-1.508115551	9.14E-117	8.84E-115	Down	[SPSK_09224] 2-oxoisovalerate dehydrogenase E1 component, beta subunit
27663386	1134	-1.503338551	7.56E-308	2.37E-305	Down	[SPSK_01178] 2-oxoisovalerate dehydrogenase E1 component, alpha subunit
27671208	1236	-11.10754403	7.09E-218	1.73E-215	Down	[SPSK_09357] GPI-anchor transamidase precursor
27665684	822	-7.060695932	7.69E-05	0.000283672	Down	[SPSK_03570] 3-ketosphinganine reductase
27665323	1728	-3.849682046	0	0	Down	[SPSK_03205] MFS transporter, PHS family, inorganic phosphate transporter
27663783	1491	-3.839327312	7.64E-17	8.93E-16	Down	[SPSK_01597] MFS transporter, DHA1 family, multidrug resistance protein
27663932	1161	-3.026967048	6.90E-07	3.45E-06	Down	[SPSK_01749] 2-hydroxyacid dehydrogenase
27672143	525	-2.570880084	1.82E-34	5.08E-33	Down	[SPSK_10468] solute carrier family 31 (copper transporter), member 1
27663245	1980	-2.370698319	0	0	Down	[SPSK_01037] malate dehydrogenase (oxaloacetate-decarboxylating) (NADP+)
27662967	1911	-2.354974996	8.64E-16	9.41E-15	Down	[SPSK_00742] ferric-chelate reductase
27669838	648	-2.202175461	8.26E-85	5.72E-83	Down	[SPSK_07908] superoxide dismutase, Fe-Mn family
27669783	870	-2.158890951	1.88E-11	1.48E-10	Down	[SPSK_07853] class II aldolase/adducin domain protein
27669193	1728	-2.104992766	1.81E-48	7.15E-47	Down	[SPSK_07252] NADPH oxidase
27669672	1038	-2.039663091	3.69E-131	4.27E-129	Down	[SPSK_07738] thiamine biosynthetic enzyme
27664428	2277	-2.036464326	3.40E-22	5.35E-21	Down	[SPSK_02279] metalloredutase
27669705	542	-1.987983983	1.07E-108	9.88E-107	Down	[SPSK_07772] short-chain dehydrogenase
27665475	1347	-1.924551321	5.95E-25	1.10E-23	Down	[SPSK_03360] MFS monocarboxylate transporter
27667950	1849	-1.846678464	0	0	Down	[SPSK_05965] urea transport protein
27670875	1599	-1.725188426	1.51E-206	3.17E-204	Down	[SPSK_09017] 2-oxoisovalerate dehydrogenase E2 component (dihydrolypoyltransacylase)
27670817	1758	-1.725170372	4.51E-42	1.51E-40	Down	[SPSK_08957] amidase
27671169	1281	-1.66783448	2.31E-271	6.16E-269	Down	[SPSK_09318] branched-chain amino acid aminotransferase
27669629	1041	-1.66238653	1.17E-33	3.18E-32	Down	[SPSK_07695] oxidoreductase, 2OG-Fe (II) oxygenase family
27663349	1422	-1.601097879	3.11E-146	4.27E-144	Down	[SPSK_01141] isopenicillin N epimerase
27662392	1350	-1.590508426	1.95E-21	2.95E-20	Down	[SPSK_00135] fumarylacetoacetase
27668443	999	-1.578487349	7.46E-168	1.17E-165	Down	[SPSK_06460] inositol oxygenase
27668333	1224	-1.537065011	3.21E-51	1.34E-49	Down	[SPSK_06350] aspergillopepsin I
27668069	1797	-1.536613527	2.08E-264	5.39E-262	Down	[SPSK_06084] 1-pyrroline-5-carboxylate dehydrogenase
27671077	1326	-1.508115551	9.14E-117	8.84E-115	Down	[SPSK_09224] 2-oxoisovalerate dehydrogenase E1 component, beta subunit
27663386	1134	-1.503338551	7.56E-308	2.37E-305	Down	[SPSK_01178] 2-oxoisovalerate dehydrogenase E1 component, alpha subunit

Ste20 is required for pathogenesis in *sporothrix schenckii*

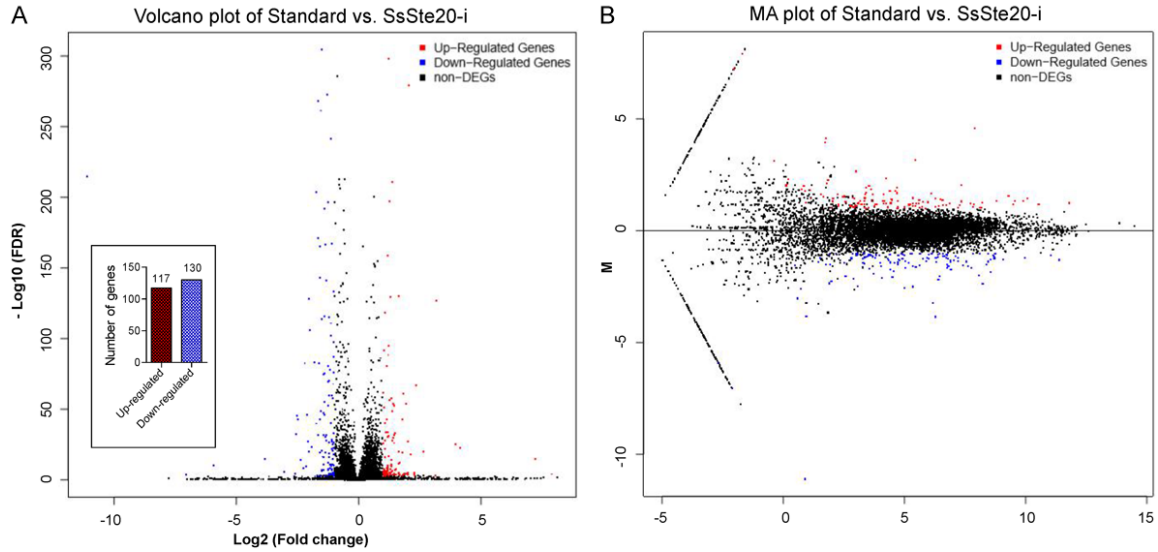


Figure 4. Global comparison of DEGs between the standard strain and the SsSte20-i mutant. A. The volcano plot of DEGs. B. The MA plot of DEGs.

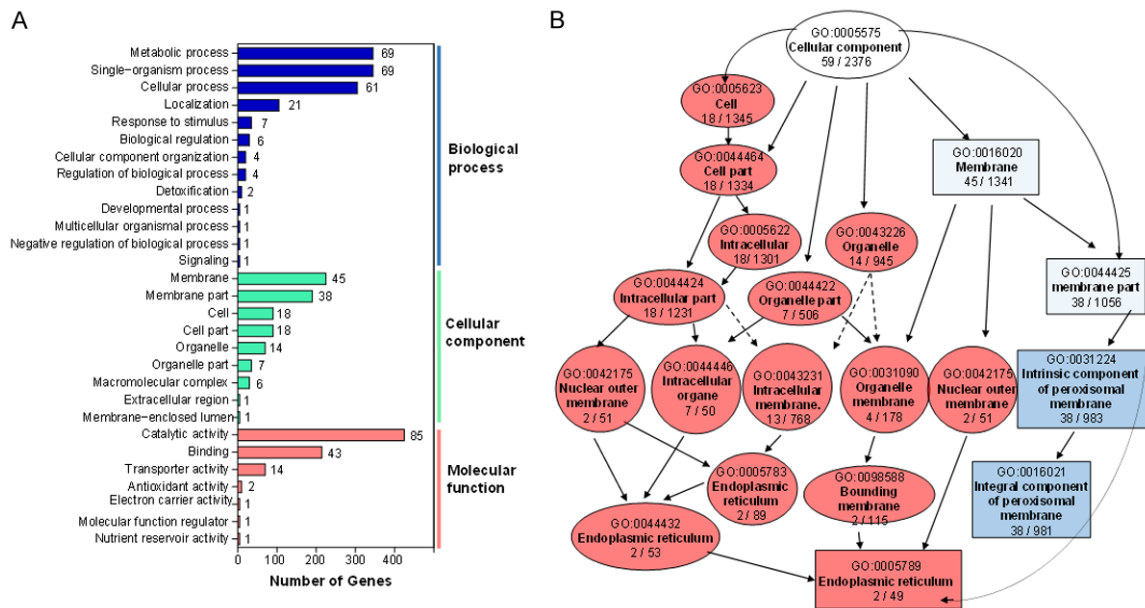


Figure 5. A. Blast2GO annotation of DEGs assigned to three GO categories (p-value below 0.05) including biological process, cellular component, and molecular function of *S. schenckii*. B. The Directed Acyclic Graph (DAG) of the DEGs assigned to the GO category of cellular component of *S. schenckii*. The blue-colored genes are down-regulated in the SsSte20-i mutant.

yeast growth form is essential for its pathogenicity; however, the mechanisms that regulate the dimorphic switching remain unclear. It may be related to osmotic pressure, partial oxygen pressure, pH value, nutritional changes and many other factors. Our previous findings [19, 21] showed that the Ste20-related kinases are involved in morphogenesis through the regula-

tion of cytokinesis and actin-dependent polarized growth. In this study, we further investigated the function of SsSte20 using dsRNAi mediated by *Agrobacterium tumefaciens*. Our results showed that inactivation of SsSte20 significantly affected the growth and internal components of *S. schenckii* conidia and impaired its dimorphic switching process. Our

Ste20 is required for pathogenesis in *sporothrix schenckii*

Table 3. The terms and genes from the function ontology that were significantly different between standard and SsSte20-i

Gene ontology term	Major identified genes	Cluster frequency	Genome frequency	P-value
Molecular function				
iron ion binding	27669629 oxidoreductase, 2OG-Fe (II) oxygenase family 27665606 methylsterol monooxygenase, ERG3; Sterol desaturase/sphingolipid hydroxylase 27669375 Cytochrome P450 family protein 27665631 2OG-Fe(II) oxygenase family oxidoreductase 27664733 C-5 sterol desaturase	10 out of 104 genes, 9.6%	54 out of 2983 genes, 1.8%	0.00121
oxidoreductase activity	27671284 leucoanthocyanidin dioxygenase 27664733 C-5 sterol desaturase 27671420 aldehyde dehydrogenase family protein 27668443 inositol oxygenase 27665954 prostaglandin-endoperoxide synthase 1	34 out of 104 genes, 32.7%	491 out of 2983 genes, 16.5%	0.00273
transition metal ion transmembrane transporter activity	27672143 copper transporter 27671735 copper transporter family protein 27671204 zinc transporter	3 out of 104 genes, 2.9%	4 out of 2983 genes, 0.1%	0.01702
Biologic process				
oxidation-reduction process	27665631 2OG-Fe(II) oxygenase family oxidoreductase 27669402 proline oxidase PrnD 27663002 aldehyde dehydrogenase (NAD (P)+) 27669193 NADPH oxidase 27669375 Cytochrome P450 family protein	32 out of 93 genes, 34.4%	469 out of 2877 genes, 16.3%	0.00218
single-organism process	27664733 C-5 sterol desaturase, ERG3; Sterol desaturase/sphingolipid hydroxylase 27667950 urea transport protein 27667431 alcohol dehydrogenase, propanol-preferring 27666281 p450; Cytochrome P450 27665606 methylsterol monooxygenase, ERG3; Sterol desaturase/sphingolipid hydroxylase	69 out of 93 genes, 74.2%	1600 out of 2877 genes, 55.6%	0.02643
Cellular component				
integral component of membrane	27664428 metalloredutase 27669193 NADPH oxidase 27667319 Regulator of G protein signaling (RGS) domain superfamily 27671735 copper transporter family protein 27664484 diacylglycerol O-acyltransferase 1 27671204 zinc transporter	38 out of 59 genes, 64.4%	981 out of 2376 genes, 41.3%	0.00970
intrinsic component of membrane	27670669 sodium-dependent phosphate transporter 27669378 mannan endo-1,6-alpha-mannosidase 27664484 diacylglycerol O-acyltransferase 1 27668084 LysP; Amino acid permease 27665323 MFS transporter, PHS family, inorganic phosphate transporter	38 out of 59 genes, 64.4%	983 out of 2376 genes, 41.4%	0.01020
membrane	27671304 HPP family, sporulation lipoprotein YhcN 27672143 copper transporter 27670367 glucan 1,3-beta-glucosidase 27665606 methylsterol monooxygenase, ERG3; Sterol desaturase/sphingolipid hydroxylase 27662888 ABC multidrug transporter	45 out of 59 genes, 76.3%	1340 out of 2376 genes, 56.4%	0.04329

study will provide a molecular basis for the development of anti-*S. schenckii* strategies targeted at SsSte20 and its related genes.

Dimorphic switching and the microbial response to environmental stress are governed by many regulatory factors that do not include only several specific genes [5, 27-29]. However, the transcriptome and regulatory network involved in dimorphic switching of *S. schenckii* remain enigmatic. We found that SsSte20 is essential

ly involved in the dimorphism of *S. schenckii* and it may be correlated with the origin and maintenance of virulence. Therefore, we compared the transcription profile of the SsSte20-i strain with that of the standard *S. schenckii* strain using the RNAseq method. Our results revealed that more than 240 genes were significantly up-regulated or down-regulated in the SsSte20-i mutant compared with the standard strain when cultured at 37°C. Many of these genes encode hypothetical proteins, which sug-

Ste20 is required for pathogenesis in *sporothrix schenckii*

gested that our understanding of dimorphism in *S. schenckii* remains largely inadequate. Among the known genes, many dehydrogenases, including formate dehydrogenase, propyl-preferring alcohol dehydrogenase, hscarg dehydrogenase, and NADH dehydrogenase, were found to be markedly up-regulated in the SsSte20-i strain compared with the standard strain. This result suggested an anaerobic growth or fermentation process in *S. schenckii*, which normally yields lactic acid, ethanol, and carbon dioxide [30]. An HPP family protein, SPSK_09455, showed homology to a sporulation lipoprotein YhcN, which is a predicted lipoprotein that had been detected as a spore protein but not a vegetative protein in *Bacillus subtilis* [31, 32]. The up-regulation of HPP family protein, SPSK_09455, in the SsSte20-i strain suggested its possible negative role in the dimorphism of *S. schenckii*. In contrast, a large number of genes were found to be down-regulated in the SsSte20-i mutant, suggesting the essential effect of SsSte20 on the global transcriptome of *S. schenckii*. For example, genes encoding metalloredoxase and Major Facilitator Superfamily (MFS) monocarboxylate transporters were found to be significantly down-regulated in the SsSte20-i strain. The MFS transporters are single-polypeptide secondary carriers capable of transporting only small solutes in response to chemiosmotic ion gradients [33]. Thus, these results suggested that inhibition of the iron/ion transport system may contribute to the dimorphic switching process in *S. schenckii*. Also, a previous study has shown that the MFS transporters were associated with G protein alpha subunit SSG-1, which is related to the stress response and fungal pathogenicity of *S. schenckii* [13].

To systematically evaluate the effects of SsSte20, we used the Gene Ontology Consortium to characterize the major effecting aspects of SsSte20 that may be associated with the dimorphism and virulence of *S. schenckii*. The results showed that 247 DEGs and 147 DEGs were found to be related to the biological process and molecular function of *S. schenckii*, respectively. Among these genes, the oxidation-reduction-related genes, such as oxidoreductase, stress-induced-phosphoprotein 1, NADH dehydrogenase, and copper/zinc superoxide dismutase (SOD); and the iron/ion-binding and transporter genes, such as ZIP zinc

transporter, copper transporter family protein, and cytochrome P450, were found to be differentially expressed in the SsSte20-i mutant. Previous studies have found that the iron/manganese SOD was related to the stress response and fungal pathogenicity of *S. schenckii* [13], nitroreductase activity was widely distributed in the *S. schenckii* complex [34], and oxidative stress occurred in rats experimentally infected by *S. schenckii*; and all of these factors contributed to the disease pathogenesis [35]. Thus, the different expression levels of these genes affected by SsSte20 inhibition may be associated with responses of *S. schenckii* to environmental stress and virulence development.

In addition to the genes associated with the biological process and molecular function of *S. schenckii*, 148 genes related to the cellular component were found to be differentially expressed in the SsSte20-i mutant. Notably, many of them are integral/intrinsic components of the membrane. The cell walls of fungi mediate all host-pathogen interactions and protect them from drastic changes in the external environment within the host [36, 37]. Researchers have found that the cell wall of *S. schenckii* is composed of glucans, galactomannans, rhamnomannans, chitin, glycoproteins, glycolipids, and melanin [38]. A proper cell wall composition is required for response to external stress and for virulence. The transcriptome analysis results obtained in this study indicated that the genes encoding glucan 1, 3-beta-glucosidase, and methylsterol monooxygenase (Sterol desaturase/sphingolipid hydroxylase), which are involved in lipid transport and metabolism of the cell wall, were affected by SsSte20 inhibition. In *Candida albicans*, β -1,3-glucan plays a role in biofilm formation and survival of biofilm-forming *Candida* to stresses [39]. This study highlighted the important role of 1, 3-beta-glucosidase in *S. schenckii*. Lipids are involved in the regulation of dimorphism and virulence of pathogenic fungi. Generally, there are certain ratios of phospholipid/ergosterol in the yeast form (less than 1) and in the mycelial form (2-20) cells in *S. schenckii*. During the transition from the yeast form to the mycelial form, phosphatidylinositol and phosphatidylserine are reduced in amount, whereas phosphatidylcholine increases [40]. In this study, we found that methylsterol monooxygenase was affected by SsSte20, and it may function as

Ste20 is required for pathogenesis in *sporothrix schenckii*

sterol desaturase/sphingolipid hydroxylase and also play an important role in the dimorphism of *S. schenckii*. Moreover, many membrane-associated transporters, such as lysine permease protein LysP, amino acid permease, MFS proteins, and ABC transporters, were found to be significantly affected by the inhibition of SsSte20. However, given the limited literature regarding the study of *S. schenckii*, their roles in dimorphic switching and pathogenesis need to be investigated in greater depth.

Acknowledgements

This study was supported by the National Natural Science Foundation of China (81502737, 81472891). This work was also supported by Liaoning Provincial Program for Top Discipline of Basic Medical Sciences, China.

Disclosure of conflict of interest

None.

Address correspondence to: Dr. Ming Li, Department of Microecology, College of Basic Medical Science, Dalian Medical University, Dalian 116044, Liaoning, China. E-mail: vivianmarat@163.com; Dr. Binbin Hou, Department of Dermatology, The Second Hospital of Dalian Medical University, Dalian 116023, Liaoning, China. E-mail: houbinbin1001@163.com

References

- [1] Chakrabarti A, Bonifaz A, Gutierrez-Galhardo MC, Mochizuki T and Li S. Global epidemiology of sporotrichosis. *Med Mycol* 2015; 53: 3-14.
- [2] Arenas R, Sánchez-Cardenas CD, Ramirez-Hobak L, Ruíz Arriaga LF and Vega Memije ME. Sporotrichosis: from KOH to molecular biology. *J Fungi (Basel)* 2018; 4.
- [3] Conceição-Silva F and Morgado FN. Immunopathogenesis of human sporotrichosis: what we already know. *J Fungi (Basel)* 2018; 4.
- [4] García Carnero LC, Lozoya Pérez NE, González Hernández SE and Martínez Álvarez JA. Immunity and treatment of sporotrichosis. *J Fungi (Basel)* 2018; 4.
- [5] Boyce KJ and Andrianopoulos A. Fungal dimorphism: the switch from hyphae to yeast is a specialized morphogenetic adaptation allowing colonization of a host. *FEMS Microbiol Rev* 2015; 39: 797-811.
- [6] Posas F, Wurgler-Murphy SM, Maeda T, Witten EA, Thai TC and Saito H. Yeast *hog1* map kinase cascade is regulated by a multistep phosphorelay mechanism in the *sln1-ypd1-ssk1* “two-component” osmosensor. *Cell* 1996; 86: 865-875.
- [7] Raitt DC, Johnson AL, Erkin AM, Makino K, Morgan B, Gross DS and Johnston LH. The *skn7* response regulator of *saccharomyces cerevisiae* interacts with *hsf1* in vivo and is required for the induction of heat shock genes by oxidative stress. *Mol Biol Cell* 2000; 11: 2335-47.
- [8] Ochiai N, Fujimura M, Motoyama T, Ichiishi A, Usami R, Horikoshi K and Yamaguchi I. Characterization of mutations in the two-component histidine kinase gene that confer fludioxonil resistance and osmotic sensitivity in the *os-1*, mutants of *neurospora crassa*. *Pest Manag Sci* 2001; 57: 437-442.
- [9] Yoshimi A, Tsuda M and Tanaka C. Cloning and characterization of the histidine kinase gene, *dic1*, from, *cochliobolus heterostrophus*, that confers dicarboximide resistance and osmotic adaptation. *Mol Genet Genomics* 2004; 271: 228-236.
- [10] Zuber S, Hynes MJ and Andrianopoulos A. G-protein signaling mediates asexual development at 25°C but has no effect on yeast-like growth at 37°C in the dimorphic fungus *penicillium marneffei*. *Eukaryot Cell* 2002; 1: 440-447.
- [11] Zuber S, Hynes MJ and Andrianopoulos A. The G-protein alpha-subunit GasC plays a major role in germination in the dimorphic fungus *penicillium marneffei*. *Genetics* 2003; 164: 487-499.
- [12] Boyce KJ, Hynes MJ and Andrianopoulos A. The Ras and Rho GTPases genetically interact to co-ordinately regulate cell polarity during development in *penicillium marneffei*. *Mol Microbiol* 2005; 55: 1487-1501.
- [13] Pérez-Sánchez L, González E, Colón-Lorenzo EE, González-Velázquez W, González-Méndez R and Rodríguez-del Valle N. Interaction of the heterotrimeric G protein alpha subunit SSG-1 of *sporothrix schenckii* with proteins related to stress response and fungal pathogenicity using a yeast two-hybrid assay. *BMC Microbiol* 2010; 10: 317.
- [14] Dan I, Watanabe NM and Kusumi A. The *ste20* group kinases as regulators of map kinase cascades. *Trends Cell Biol* 2001; 11: 220-230.
- [15] Boyce KJ and Andrianopoulos A. Ste20-related kinases: effectors of signaling and morphogenesis in fungi. *Trends Microbiol* 2011; 19: 400-410.
- [16] Atkins BD, Yoshida S, Saito K, Wu CF, Lew DJ and Pellman D. Inhibition of *cdc42* during mitotic exit is required for cytokinesis. *J Cell Biol* 2013; 202: 231-240.
- [17] Zhang Z, Hou B, Xin Y and Liu X. Protein profiling of the dimorphic pathogenic fungus, *sporothrix schenckii*.

Ste20 is required for pathogenesis in *sporothrix schenckii*

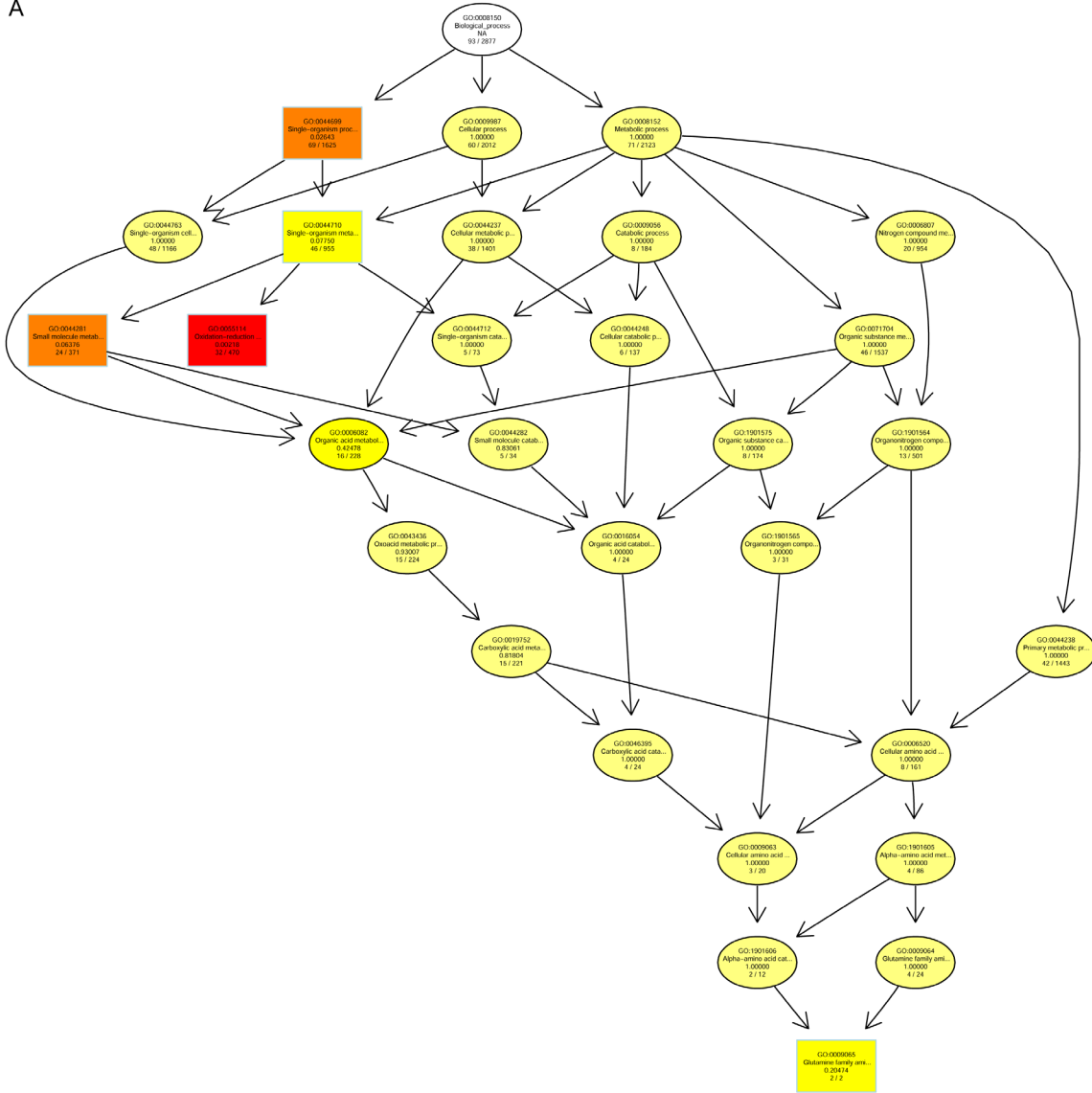
- thrix schenckii. *Mycopathologia* 2012; 173: 1-11.
- [18] Zhang Z, Hou B, Wu YZ, Wang Y, Liu X and Han S. Two-component histidine kinase DRK1 is required for pathogenesis in *sporothrix schenckii*. *Mol Med Rep* 2018; 17: 721-728.
- [19] Zhang Z, Hou B, Zheng F, Yu X and Liu X. Molecular cloning, characterization and differential expression of a *sporothrix schenckii* STE20-like protein kinase SsSte20. *Int J Mol Med* 2013; 31: 1343-1348.
- [20] Rodriguez-Caban J, Gonzalez-Velazquez W, Perez-Sanchez L, Gonzalez-Mendez R and Rodriguez-del Valle N. Calcium/calmodulin kinase1 and its relation to thermotolerance and HSP90 in *sporothrix schenckii*: an RNAi and yeast two-hybrid study. *BMC Microbiol* 2011; 11: 162.
- [21] Zhang Z, Hou B, Wu YZ, Wang Y, Liu X and Han S. Two-component histidine kinase DRK1 is required for pathogenesis in *sporothrix schenckii*. *Mol Med Rep* 2018; 17: 721-728.
- [22] Liu X, Zhang Z, Hou B, Wang D, Sun T, Li F, Wang H and Han S. Rapid identification of *sporothrix schenckii* in biopsy tissue by PCR. *J Eur Acad Dermatol Venereol* 2013; 27: 1491-1497.
- [23] Garrison RG, Boyd KS and Mariat F. Ultrastructural studies of the mycelium-to yeast transformation of *sporothrix schenckii*. *J Bacteriol* 1975; 124: 959-968.
- [24] Wang F, Tao J, Qian Z, You S, Dong H, Shen H, Chen X, Tang S and Ren S. A histidine kinase PmHHK1 regulates polar growth, sporulation and cell wall composition in the dimorphic fungus *penicillium marneffeii*. *Mycol Res* 2009; 113: 915-923.
- [25] Yang X, Teng K, Zhang J, Wang F, Zhang T, Ai G, Han P, Bai F and Zhong J. Transcriptome responses of *lactobacillus acetotolerans* F28 to a short and long term ethanol stress. *Sci Rep* 2017; 7: 2650.
- [26] Conesa A and Götz S. Blast2Go: a comprehensive suite for functional analysis in plant genomics. *Int J Plant Genomics* 2008; 2008: 619832.
- [27] Liu H, Xi L, Zhang J, Li X, Liu X, Lu C and Sun J. Identifying differentially expressed genes in the dimorphic fungus *penicillium marneffeii* by suppression subtractive hybridization. *FEMS Microbiol Lett* 2007; 270: 97-103.
- [28] Boyce KJ, Schreider L, Kirszenblat L and Andrianopoulos A. The two-component histidine kinases DrkA and SlnA are required for in vivo growth in the human pathogen *penicillium marneffeii*. *Mol Microbiol* 2011; 82: 1164-1184.
- [29] Boyce KJ, Cao C and Andrianopoulos A. Two-component signaling regulates osmotic stress adaptation via SskA and the high-osmolarity glycerol MAPK pathway in the human pathogen *talaromyces marneffeii*. *mSphere* 2016; 1.
- [30] Meinhof W and Marghescu S. On the electrophoretic demonstration of isoenzymes of lactate dehydrogenase, malate dehydrogenase and glucose-6-phosphate dehydrogenase in dermatophytes, *scopulariopsis brevicaulis* and *sporotrichum schenckii*. *Arch Klin Exp Dermatol* 1969; 234: 25-35.
- [31] Bagyan I, Noback M, Bron S, Paidhungat M and Setlow P. Characterization of yhcn, a new forespore-specific gene of *bacillus subtilis*. *Gene* 1998; 212: 179-188.
- [32] Marchler-Bauer A, Bo Y, Han L, He J, Lanczycki CJ, Lu S, Chitsaz F, Derbyshire MK, Geer RC, Gonzales NR, Gwadz M, Hurwitz DI, Lu F, Marchler GH, Song JS, Thanki N, Wang Z, Yamashita RA, Zhang D, Zheng C, Geer LY and Bryant SH. Cdd/sparcle: functional classification of proteins via subfamily domain architectures. *Nucleic Acids Res* 2017; 45: D200-D203.
- [33] Pao SS, Paulsen IT and Saier MH Jr. Major facilitator superfamily. *Microbiol Mol Biol Rev* 1998; 62: 1-34.
- [34] Stopiglia CD, Carissimi M, Daboit TC, Stefani V, Corbellini VA and Scroferneker ML. Application of 6-nitrocoumarin as a substrate for the fluorescent detection of nitroreductase activity in *sporothrix schenckii*. *Rev Inst Med Trop Sao Paulo* 2013; 55: 353-356.
- [35] Castro VSP, Da Silva AS, Thomé GR, Wolkmer P, Castro JLC, Costa MM, Graça DL, Oliveira DC, Alves SH, Schetinger MRC, Lopes STA, Stefani LM, Azevedo MI, Baldissera MD and Andrade CM. Oxidative stress in rats experimentally infected by *sporothrix schenckii*. *Microb Pathog* 2017; 107: 1-5.
- [36] Harris M, Mora-Montes HM, Gow NA and Coote PJ. Loss of mannosylphosphate from *Candida albicans* cell wall proteins results in enhanced resistance to the inhibitory effect of a cationic antimicrobial peptide via reduced peptide binding to the cell surface. *Microbiology* 2009; 155: 1058-1070.
- [37] Mora-Montes HM, Ponce-Noyola P, Villagómez-Castro JC, Gow NA, Flores-Carreón A and López-Romero E. Protein glycosylation in *Candida*. *Future Microbiol* 2009; 4: 1167-1183.
- [38] Lopes-Bezerra LM, Walker LA, Niño-Vega G, Mora-Montes HM, Neves GWP, Villalobos-Duno H, Barreto L, Garcia K, Franco B, Martínez-Álvarez JA, Munro CA and Gow NAR. Cell walls of the dimorphic fungal pathogens *sporothrix schenckii* and *sporothrix brasiliensis* exhibit bilaminar structures and sloughing of extensive and intact layers. *PLoS Negl Trop Dis* 2018; 12: e0006169.

Ste20 is required for pathogenesis in *sporothrix schenckii*

- [39] Tan Y, Ma S, Leonhard M, Moser D and Schneider-Stickler B. β -1,3-glucanase disrupts biofilm formation and increases antifungal susceptibility of *Candida albicans* day185. *Int J Biol Macromol* 2018; 108: 942-946.
- [40] Kitajima Y. Structural and biochemical characteristics of pathogenic fungus: cell walls, lipids and dimorphism, and action modes of antifungal agents. *Nihon Ishinkin Gakkai Zasshi* 2000; 41: 211-217.

Ste20 is required for pathogenesis in *Sporothrix schenckii*

A



Ste20 is required for pathogenesis in *Sporothrix schenckii*

B

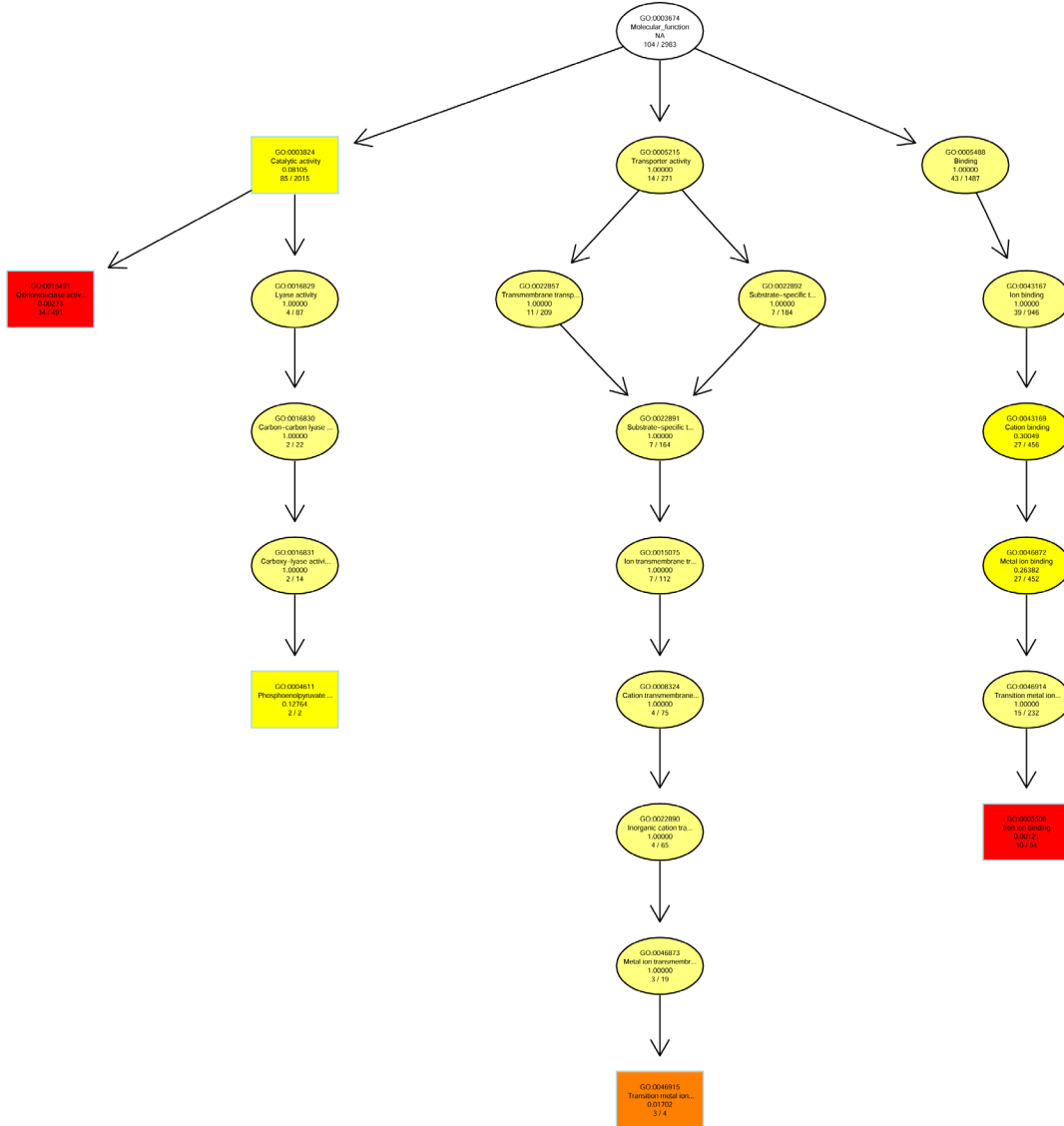


Figure S1. A. DEGs involved in biological process. B. DEGs involved in molecular_function.